Soft X-Ray Resonant Magnetic Scattering from a Magnetically Coupled Ag/Ni Multilayer

J. M. Tonnerre,[1] L. Sève,[1] D. Raoux,[1] G. Soullié,[2,3] B. Rodmacq,[4] and P. Wolfers[1]

[1]*Laboratoire de Cristallographie, Centre National de la Recherche Scientifique, Université J. Fourier, B.P. 166, 38042 Grenoble Cédex 09, France*

[2]*Laboratoire de Chimie-Physique, Centre National de la Recherche Scientifique, Université Pierre et Marie Curie, 11 rue Pierre et Marie Curie, 75231 Paris Cedex 05, France*

[3]*Laboratoire pour l'Utilisation du Rayonnement Electromagnétique, Centre National de la Recherche Scientifique, Commissariate à l'Energie Atomique, MESR, Bât 209D, Centre Universitaire Paris-Sud, 91405 Orsay Cedex, France*

[4]*Commissariate à l'Energie Atomique, DRFMC, SP2M-MP, BP 85, 38054 Grenoble Cedex 9, France*

(Received 27 February 1995)

X-ray resonant magnetic scattering experiments using linear and circular polarized light were performed at the Ni $L_{2,3}$ absorption edges on a Ag/Ni multilayer. A superlattice magnetic peak, due to the antiferromagnetic coupling between Ni layers, is evidenced. In the case of a ferromagnetic coupling, large changes in the charge peak (up to 15%) are observed upon reversal of the direction of the magnetic field. The magnetic scattering amplitude is evaluated to $8r_0$ per nickel atom. Sum rules have been applied for the first time to the energy-dependent magnetic amplitude.

PACS numbers: 75.50.Rr, 75.70.Fr, 78.70.Ck

Since the observation of a huge resonant enhancement for the x-ray magnetic scattering cross section near an absorption threshold in rare earths [1] and actinides [2], x-ray magnetic scattering has become a new experimental technique for the investigation of magnetic materials. For a $3d$ transition metal, a large enhancement is predicted to occur at the $L_{2,3}$ absorption edges [3]. Such an effect has been observed by specular reflectivity at Fe and Co edges for a 35 Å Fe(110) single crystal film [4] and recently for a buried Co thin layer [5]. Although the energies of the $L_{2,3}$ absorption edges of $3d$ transition metals do not allow diffraction experiments for regular crystalline materials, such experiments can be carried out for artificial materials with long periods, such as multilayers or superlattices. Moreover, metallic multilayers show outstanding magnetic properties and are, therefore, extensively under consideration [6].

In this Letter, we report on an x-ray resonant magnetic scattering (XRMS) experiment performed at the Ni $L_{2,3}$ edges in a magnetically coupled Ag/Ni multilayer. Magnetization and neutron scattering measurements [7,8] have shown, for an 11 Å Ag thickness, an in-plane antiferromagnetic coupling between Ni layers. They can be ferromagnetically coupled by applying a magnetic field. It is thus possible to perform XRMS in both the antiferro- (AF) and the ferromagnetic (F) coupling cases. Our first goal is to demonstrate the possibility to evidence an AF coupling in the multilayer by XRMS throughout the appearance of a magnetic superlattice diffraction peak and to quantify the resonant magnetic scattering amplitude. Our second motivation is to test the possibility of using XRMS as a spectroscopic technique like x-ray magnetic circular dichroism (XMCD). Indeed, the expression of XMCD is readily identified with the imaginary part of XRMS [9].

The experiments were conducted on the SB3 station [10] at LURE using the synchrotron radiation from the Super ACO storage ring. This bending magnet beam line incorporates in a vacuum chamber (10^{-5}–10^{-6} Torr) a fixed exit two-crystal monochromator and a two-circle diffractometer both with horizontal axes. Beryl crystals have been used to cover the Ni $L_{2,3}$ absorption edges (853, 870.3 eV) range with a good energy resolution (0.3 eV). In the case of the AF coupling, the diffraction experiments were performed using the linearly polarized beam radiated in the midplane of the storage ring orbit with a degree of linear polarization of 99%. In the case of the F coupling, a circularly polarized beam [$\tau_c = (47 \pm 2)\%$] had to be used in order to enhance the magnetic effect by coupling the regular Thomson scattering and the resonant magnetic one. This was achieved by moving out of the midplane by 0.48 ± 0.3 mrad.

The Ag/Ni multilayer has been prepared by dc sputtering onto a glass substrate kept at 100 K during the depositon process [11]. The Ag layers are 11 Å thick and the thickness of the Ni ones, 17.5 Å, has been chosen so that the magnetic saturation field (600 G) [7] is in the range of our magnetic device and that the Curie temperature (~610 K) [12] is as high as that of bulk Ni, since our scattering measurements could be performed only at room temperature. The sample was magnetized *in situ* by a permanent $SmCo_5$ magnet located above it on a rotation stage. The magnetization of the sample could thus be rotated by 360° in the plane of the multilayer. The intensity of the applied magnetic field was set by adjusting the distance between the magnet and sample.

The total elastic x-ray scattering factor is given by $f = -(\hat{\mathbf{e}}_f^* \cdot \hat{\mathbf{e}}_f)(f_0 + f' - if'') + f_{\mathrm{mag}}^{\mathrm{res}}$, where $f_0 + f'$ and if' are the real and imaginary parts of the atomic form factor, respectively. The resonant magnetic scattering factor $f_{\mathrm{mag}}^{\mathrm{res}}$ is due to an electronic transition from an inner shell electron into available empty electronic states. Sensitivity to magnetization arises from the ef-

 0031-9007/95/75(4)/740(4)$06.00

fects of the spin-orbit interaction in the core level and of the spin polarization of the conduction band [3]. Its amplitude is governed by the F_{LM} transition probabilities, where L is the order of the transition and M is the change in angular momentum. These coefficients contain matrix elements, which couple the ground state to the excited magnetic levels, and a resonant energy denominator. In the present case, we consider only electric dipolar transitions $2p_{3/2(1/2)} \rightarrow 3d_{5/2(3/2)}$ so that $f_{\text{mag}}^{\text{res}}$ is proportional to $[F_{1,1} - F_{1,-1}]$. Therefore, the resonant magnetic scattering amplitude, which depends on the magnetization direction of the local moment $\hat{\mathbf{z}}_j$ on site j and on the polarizations $\hat{\mathbf{e}}_f$ and $\hat{\mathbf{e}}_i$ of the scattered and incident photon beams, can be written in units of r_0 as [3]

$$f_{\text{mag}}^{\text{res}} = -i(\hat{\mathbf{e}}_f^* \times \hat{\mathbf{e}}_i)\cdot\hat{\mathbf{z}}_j n_m \frac{x + i}{1 + x^2}. \quad (1)$$

In formula (1), we follow the formalism used by de Bergevin *et al.* [13], where the resonant energy-dependent factor has been put apart from the magnetic amplitude n_m. We assume a Lorentzian dependence of $x = [(E_f - E_i) - \hbar\omega]/(\Gamma/2)$, the relative energy deviation from the resonance. $E_f - E_i$ is the transition energy, $\hbar\omega$ is the energy of the incident photons, and Γ is the total width of the excited state.

In the AF case, we expect a purely magnetic peak to occur at $q = \pi/\Lambda$, Λ being the period of the multilayer. In the F one, XRMS leads to a magnetic contribution to the charge reflections. To bring it out, we derive an asymmetry ratio $R_a = (I^{\uparrow} - I^{\downarrow})/(I^{\uparrow} + I^{\downarrow})$, where $I^{\uparrow}$ and $I^{\downarrow}$ are the diffracted intensities for the two opposite directions of the applied magnetic field parallel to both the plane of the layers and the diffraction plane. In our configuration (diffraction in the vertical plane, with a circularly polarized beam), R_a is given by

$$R_a = \frac{4\cos^3(\theta)\tau^{1/2}(F_r M_r - F_i M_i)}{[1 + \tau\cos^2(2\theta)]|F^2| + \cos^2(\theta)(1 + \tau)|M|^2}, \quad (2)$$

where τ is the ratio of the vertically and horizontally polarized intensities, θ is the Bragg angle, and F and M are the complex charge and magnetic structure factors of the multilayer, respectively,

$$F_r + iF_i = \sum_{\text{Ni,Ag}} f_j e^{i\mathbf{k}\cdot\mathbf{r}_j}, \quad M_r + iM_i = \sum_{\text{Ni}} f_{\text{mag}\,j}^{\text{res}} e^{i\mathbf{k}\cdot\mathbf{r}_j},$$

with

$$f_{\text{mag}}^{\text{res}} = \frac{x + i}{1 + x^2} n_m(L_3) + \frac{y + i}{1 + y^2} n_m(L_2), \quad (3)$$

where x and y stand for the relative deviations from resonances at the L_3 and L_2 edges, respectively.

Figure 1 displays a sequence of $\theta/2\theta$ diffraction patterns collected at various energies near the Ni L_3 absorption edge. The peak corresponding to the chemical modulation of the sample ($\Lambda = 28.5$ Å) is observed around $\theta = 15°$. Another peak is clearly found at a scattering angle around $\theta = 7.5°$ when the x-ray photon energy is tuned right at the Ni L_3 absorption edge. Its position results from the doubling of the chemical periodicity due to the AF coupling between Ni layers. Figure 1 also evidences strong intensity changes and angular shifts of the chemical modulation peak. We used them to get a direct measurement of the f' and f'' optical constants for Ni in the multilayer in the vicinity of the L_3 and L_2 edges where tabulated data are not reliable. The width of the Bragg peak is related to the thickness probed by the incident photons and directly measures the absorption coefficient. The huge shifts of the Bragg peak are related not only to the changes in the x-ray wavelength but mainly to strong changes in the refraction index and they allow one to extract the f' values for the Ni atoms. Kramers-Kronig and inverse Kramers-Kronig relationships have been used successfully to check the consistency of the independently measured f' and f'' values. It appears that the amplitude of the variation of f' near the L_3 Ni absorption edge reaches a high value of -60 electrons. A detailed report on the f' and f'' measurements will be published elsewhere [14].

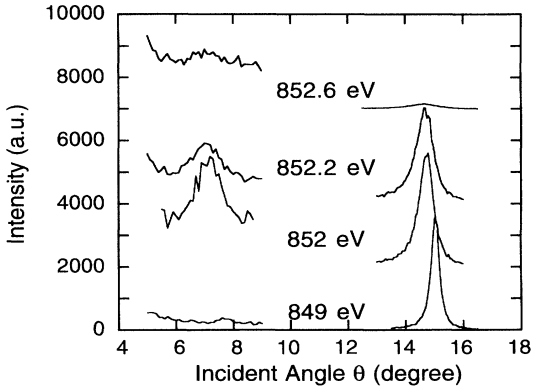

FIG. 1. Diffraction patterns of a Ag/Ni multilayer for different energies around the Ni L_3 absorption edge using a linearly polarized beam. The intensity of the AF peak (see text) has been scaled by a factor of 50. The various curves have been vertically shifted by 2000, 4000, and 7000, respectively.

The energy dependence through the L_3 absorption edge of the integrated intensity of the AF peak, corrected for absorption, is shown in Fig. 2. Above 852.6 eV, the weakness of the XRMS amplitude and the strong absorption both prevent measurement of the AF peak which smears out in the increasing background. Its intensity at maximum is about 3% of that of the multilayer first-order charge peak. Taking into account the Lorentz factor and assuming a random distribution of the direction of the magnetic moments in the AF domains, a n_m value of $(7.5 \pm 1.4)r_0$ at the L_3 edge has been extracted from the ratio of the AF integrated intensity to that of the chemical modulation peak. We point out that such a high

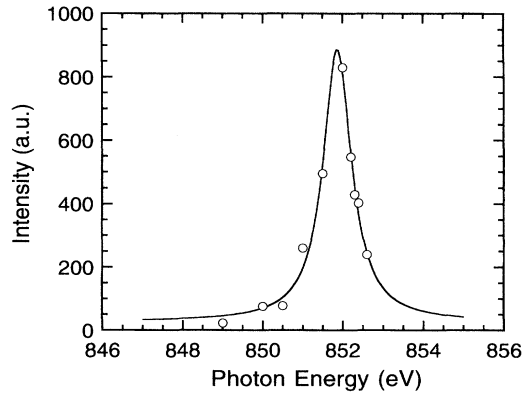

FIG. 2. Integrated intensity of the AF peak (corrected for absorption) vs incident photon energy at the Ni L_3 edge. The solid line is a Lorentzian fit.

value of the Ni magnetic amplitude represents 27% of its atomic scattering factor.

In a second part, by using data obtained in the F case, we aim to exploit for the first time the capability of XRMS to give information similar to that derived from XMCD, in particular to give an independent measurement of the spin and orbital contributions to the magnetic moment by applying the sum rules [15,16].

Figure 3 shows R_a measured as a function of photon energy near the L_3 and L_2 Ni absorption edges. At each energy, the intensities have been registered at the top of the multilayer diffraction peak for the two opposite directions of the applied magnetic field, with right-handed circularly polarized x rays. An R_a value as high as 15% is observed. We have attempted to fit the experimental

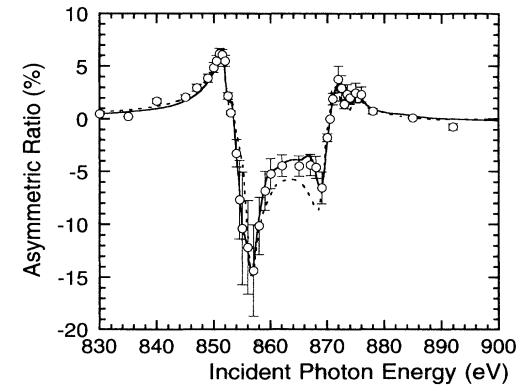

FIG. 3. Asymmetry ratio of the chemical modulation diffraction peak in the vicinity of the L_3 and L_2 edges for a Ag/Ni multilayer. The diffraction experiment is performed in the vertical geometry using a circularly polarized beam. The dashed curve is a simulation assuming Lorentzian magnetic resonances while the solid curve is calculated from the fit of the M_r and M_i magnetic structure factors (see text).

R_a using Eq. (2). Calculated values have been used for τ. The f' and f'' values have been determined as mentioned above. The crystallographic data which are needed to calculate the F and M structure factors have been determined from our diffraction spectra and from a previous extensive diffraction work [17]. The parameters E, Γ, and n_m, which define the Lorentzian resonances, are the only ones which have been adjusted at both edges. The dashed line in Fig. 3 shows that a reasonable agreement between the calculated R_a and the data has been achieved. We included in this simulation the L_3 and L_2 resonances and two weaker ones at ~4 eV above the L_3 and L_2 edges in order to account for the weak features in the bulk Ni XMCD, reported by Chen *et al.* [18]. Above the L_2 edge, such a feature is clearly evidenced in our data as a shoulder in R_a (Fig. 3) at the right energy. At the L_3 and L_2 edges, the magnetization-dependent amplitudes n_m have been adjusted to $(7.8 \pm 0.4)r_0$ and $(-2.9 \pm 0.4)r_0$, respectively. We stress that the L_3 edge value is in good agreement with that obtained using the AF peak.

This XRMS analysis enables us to extract the real and imaginary parts of the resonant magnetic amplitude ($f_{\mathrm{mag}}^{\mathrm{res}}$) given by Eq. (3) and then, by using sum rules, to try to separate out the spin and orbital contributions. However, as shown in Fig. 3, the Lorentzian assumption for the four resonances does not allow proper fitting of the data between the L_3 and L_2 edges. Therefore we try to extract $f_{\mathrm{mag}}^{\mathrm{res}}$ directly following an iterative method. Assuming initially M_i equal to 0, we first calculate M_r from Eq. (2), and thus the real part of $f_{\mathrm{mag}}^{\mathrm{res}}$. Then, by using the Kramers-Kronig relationship, we get its imaginary part $\mathrm{Im}(f_{\mathrm{mag}}^{\mathrm{res}})$. We recalculate M_r by introducing the new value for M_i in Eq. (2) and we repeat the process until a stable solution is reached for both the real and imaginary parts of $f_{\mathrm{mag}}^{\mathrm{res}}$. The solid line in Fig. 3 is calculated using these values. In Fig. 4, we compare $\mathrm{Im}(f_{\mathrm{mag}}^{\mathrm{res}})$ derived in such a way to the XMCD dichroic

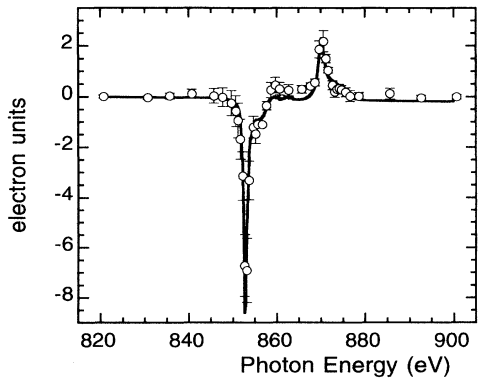

FIG. 4. Imaginary part of XRMS (open circles) and MCD spectrum (solid line) for Ni in electron units. The MCD data are from Sainctavit *et al.* [18].

signal measured in an absorption experiment for bulk Ni [19]. Both results are in good general agreement. This demonstrates that XRMS may be used as a spectroscopic technique like XMCD. However, weak discrepancies are found, especially between the L_3 and L_2 edges where a positive XRMS derived signal is observed. Since our simulations show that R_a values are sensitive to the f' and f'' parameters, we used as a test an independent set of f' and f'' values derived from an absorption measurement on bulk Ni and we obtain the same positive R_a values between the L_3 and L_2 edges. In a recent paper, O'Brien *et al.* also noticed a weak XMCD signal between the L_3 and L_2 edges for bulk Ni and Co and ascribed it to diffuse magnetism related to the s-electron levels [20]. However, for bulk phases, these features are negative. At this stage, we have no clear indication that the positive signal that we measured is related to the thinness of the Ni layers (8 ML) sandwiched between Ag ones. It may as well be related to small systematic errors in our measurements or in the data processing.

Finally, although the atomic dichroism sum rules are still a matter of controversy for $3d$ transition metals, we applied them to the imaginary part of the resonant magnetic scattering. We first determined the $\langle L_z\rangle/\langle S_z\rangle$ ratio, which is the most accepted parameter that can be derived from sum rules [21,22]. Neglecting the magnetic dipolar operator [16], we obtain a value ranging from 0.2 to 0.3 depending on the integration limit for the L_3 (and L_2) edge in between both edges. The lower value is comparable to Ni bulk XMCD published results [18,23]. We then try to separately evaluate $\langle L_z\rangle$ and $\langle S_z\rangle$. Using $n_h = 1.6$ as the number of holes in the d band [24,25], the orbital sum rule gives $\langle L_z\rangle = (0.044 \pm 0.01)\mu_B$ and the spin one leads to $2\langle S_z\rangle = (0.37 \pm 0.06)\mu_B$. The sum yields the total magnetic moment $M_T = (0.42 \pm 0.07)\mu_B$ which is in reasonable agreement with the one derived from magnetization measurements: For a 17 Å Ni thickness, the saturation magnetization per atom is $0.57\mu_B$ at 5 K [12] and is reduced to about $(0.49 \pm 0.02)\mu_B$ at room temperature [26].

To summarize, this work evidences a huge enhancement of the magnetic x-ray scattering cross section of a transition metal like Ni when the incident soft x-ray energy is set near its $L_{2,3}$ absorption edges. In that case, XRMS allows one to easily observe a magnetic diffraction peak due to the AF coupling between Ni layers in a Ag/Ni multilayer. Experiments performed with both F and AF coupling yield consistent values of the magnetization dependent amplitude, which is about $8r_0$ at the L_3 edge. Applying sum rules to the imaginary part of the resonant magnetic amplitude, which can be directly determined from the XRMS intensity, it is possible to separate the orbital and spin components of the magnetic moment. Evidently, we have to face the same difficulties in using the sum rules as those encountered using XMCD data. Moreover, such a separation seems to be easier using XMCD which does not mix up the real and imaginary parts of the magnetic scattering. However, in the soft x-ray energy range, absorption measurements using electron detection are restricted to the very near surface and, due to surface oxidation problems, the use of this technique may be difficult for samples which are not prepared *in situ* as we actually found out. Alternatively, the use of fluorescence detection shows severe limitations as recently demonstrated [27]. Furthermore, XMCD does not allow investigation of antiferromagnetically coupled multilayers. We also point out that, being species selective, XRMS should allow one to probe the magnetism of each component in more complicated structures like multilayers of alloys, which neutron scattering does not. In conclusion, the development of a photon-in–photon-out technique like XRMS might be fruitful to study eventual modifications of magnetic properties of elements in two-dimensional artificial structures.

We would like to thank F. de Bergevin and G. Krill for stimulating discussions and P. Sainctavit for providing us with Ni XMCD data.

[1] D. Gibbs *et al.*, Phys. Rev. Lett. **61**, 1241 (1988); D. Gibbs *et al.*, Phys. Rev. B **43**, 5663 (1991).
[2] E. D. Isaacs *et al.*, Phys. Rev. Lett. **62**, 1671 (1989); D. B. McWhan *et al.*, Phys. Rev. B **42**, 6007 (1990).
[3] J. P. Hannon *et al.*, Phys. Rev. Lett. **61**, 1245 (1988); Phys. Rev. Lett. **62**, 2644(E) (1989).
[4] C. C. Kao *et al.*, Phys. Rev. Lett. **65**, 373 (1990).
[5] C. C. Kao *et al.*, Phys. Rev. B **50**, 9599 (1994).
[6] *Proceedings of the International Symposium on Magnetic, Ultra Thin Films, Multilayers and Surfaces*, edited by G. Bayreuther and F. S. A. de Broeder [J. Magn. Magn. Mater. **121** (1993)].
[7] C. A. Dos Santos *et al.*, Appl. Phys. Lett. **59**, 126 (1991).
[8] B. Rodmacq *et al.*, Europhys. Lett. **15**, 503 (1991).
[9] P. Carra *et al.*, Phys. Rev. Lett. **64**, 1286 (1990).
[10] R. Barchewitz *et al.*, Rev. Phys. Appl. **23**, 1661 (1988).
[11] B. Rodmacq *et al.*, J. Phys. Condens. Matter **2**, 95 (1990).
[12] B. Rodmacq *et al.*, J. Magn. Magn. Mater. **104-107**, 1739 (1992).
[13] F. de Bergevin *et al.*, Phys. Rev. B **46**, 10 772 (1992).
[14] L. Sève *et al.* (unpublished).
[15] B. T. Thole *et al.*, Phys. Rev. Lett. **68**, 1943 (1992).
[16] P. Carra *et al.*, Phys. Rev. Lett. **70**, 694 (1993).
[17] B. Rodmacq, J. Appl. Phys. **70**, 4194 (1991).
[18] C. T. Chen *et al.*, Phys. Rev. B **43**, 6785 (1991).
[19] P. Sainctavit *et al.*, J. Appl. Phys. **72**, 1985 (1992).
[20] W. L. O'Brien *et al.*, Phys. Rev. B **50**, 12 672 (1994).
[21] C. T. Chen *et al.*, Phys. Rev. Lett. **75**, 152 (1995).
[22] R. Wu *et al.*, Phys. Rev. Lett. **73**, 1994 (1994).
[23] J. Vogel *et al.*, Phys. Rev. B **49**, 3230 (1994).
[24] E. Wimmer *et al.*, Phys. Rev. B **30**, 3113 (1984).
[25] S. C. Hong *et al.*, Phys. Rev. B **39**, 5719 (1989).
[26] B. Rodmacq *et al.*, Physica (Amsterdam) **180&181B**, 477 (1992).
[27] L. C. Duda *et al.*, Phys. Rev. B **50**, 16 758 (1994).